ISSN 0018-151X, High Temperature, 2008, Vol. 46, No. 6, pp. 746–751. © Pleiades Publishing, Ltd., 2008.
Original Russian Text © E.N. Vasil'ev, D.A. Nesterov, 2008, published in Teplofizika Vysokikh Temperatur, Vol. 46, No. 6, 2008, pp. 814–819.

PLASMA INVESTIGATIONS

Numerical Simulation of the Spatial Structure of a Moving Arc Discharge

E. N. Vasil'ev and D. A. Nesterov

Institute of Computational Modeling, Siberian Division, Russian Academy of Sciences, Krasnoyarsk, 660036 Russia

Received September 25, 2007

Abstract—Results are given of the calculation of the structure of an arc discharge moving on parallel electrodes in air under the effect of a transverse magnetic field (0.086 T) at a current strength of 320 A. The numerical simulation is performed within an unsteady-state three-dimensional mathematical model of radiation magnetogasdynamics. The calculations reveal that fluctuations of values of physical parameters and of spatial shape of arc arise in the arc, which are caused by the gas flow past the discharge column and by unsteady-state processes in the electrode regions. Comparison is made with the available experimental data.

PACS numbers: 52.80.Mg

DOI: 10.1134/S0018151X08060023

INTRODUCTION

The simulation of dynamics of discharges in gas flows is associated with the need for inclusion of a whole complex of physical mechanisms such as electromagnetic and gasdynamic interactions, radiation, and heat conduction. The correct inclusion of these mechanisms in a computational model is quite complex and ambiguous; therefore, of great interest in simulating discharges are the results of experimental investigations aimed at determining the discharge structure and measuring the local characteristics of gas-discharge plasma. Comparison of theoretical and experimental data enables one to estimate the adequacy of description of real physical processes by the mathematical model, and simulation results make it possible to obtain a large body of additional useful information about the process being investigated. The dynamics of discharge formation are most significantly affected by the current strength I and magnetic field induction B, because the parameter I defines the power of energy release in the discharge, and the intensity of force interaction between discharge and gas flow is characterized by the product IB. Depending on the order of magnitude of the quantities I and B, different physical factors may predominate in the discharge dynamics; therefore, calculations in a wide range of parameters enable one to obtain more complete information about special features of the process of discharge formation and to test the computational model under different conditions of interaction.

The mode of strong interaction of discharge in a flow was investigated by Kukhtetskii et al. [1], who found that intensive interaction between a high-current discharge and gas flow (I = 20 kA, B = 0.6 T) is a significantly unsteady-state process characterized by chaotic variation of the structure of gas-discharge region. The division of discharge into several current-conducting channels was quite frequently observed in such experiments with molecular gases; the reason for this was not found in [1]. Numerical two-dimensional simulation of the process resulted in obtaining the discharge dynamics which were qualitatively similar to those observed experimentally; it was further found that the reason for the division of the discharge region is the development of Rayleigh–Taylor instability (RTI) [2]. The calculated maximal value of temperature in discharge could be as high as 2×10^4 K; in so doing, the principal mechanism of energy loss was radiation. The discharge structure in experiments was determined by photographs from different aspect angles, and the local characteristics of the discharge were not measured; therefore, no quantitative comparison of theoretical and experimental data could be performed.

Sebald [3] gives the results of investigation by optical methods of the discharge structure for low values of current strength ($I \approx 20$ A) and magnetic field induction ($B \approx 1.5 \times 10^{-3}$ T). A two-dimensional distribution of temperature was experimentally obtained for the cross section of discharge with the maximal value of approximately 7×10^3 K. The recovered velocity field indicates that two symmetric eddies swirling in opposite directions are formed in the discharge. The numerical investigation of this process involved the use of three-dimensional computational model of radiation magnetogasdynamics which included heat transfer of gas to the electrode surface [4]. Comparison of the experimental and calculation results revealed that the model adequately describes the characteristic features of the process, with the difference in temperature values amounting to approximately 5%. The calculations

revealed that the principal mechanism of energy loss in the discharge column is heat conduction, and the formation of meniscus-like shape of discharge cross section is caused by the vortex motion of gas. The heat transfer between gas and electrodes leads to the thermal contraction of discharge and to the increase in current density at the electrode surface and in the zone of spreading. The gas temperature here is much higher ($T \approx 1.2 \times 10^4$ K) than in the discharge column; as a result, the effect of radiation in the energy balance becomes significant. In contrast to the case of high-current discharge, no development of RTI was observed.

The experimental data in the intermediate range of interaction intensity are given by Slovetskii [5], who used spectral methods for obtaining the temperature distribution in an electric arc moving on parallel electrodes in air at atmospheric pressure and current strength of 320 and 1700 A, with the respective values of transverse magnetic field intensity being 6.85×10^4 and 3.2×10^4 A/m, respectively. Slovetskii [5] estimated the error of measurement of temperature in discharge at 10% or less.

The present paper deals with the simulation of discharge dynamics for the conditions of the latter experiment.

FORMULATION OF THE PROBLEM

The simulation of the process of interaction between a discharge and a gas flow in a channel of constant rectangular cross section involved the use of the following unsteady-state three-dimensional mathematical model of radiation magnetogasdynamics:

$$\frac{\partial \mathbf{U}}{\partial t} + \frac{\partial \mathbf{E}}{\partial x} + \frac{\partial \mathbf{F}}{\partial y} + \frac{\partial \mathbf{G}}{\partial z} = \mathbf{S},$$

$$\mathbf{U} = (\rho, \rho u, \rho v, \rho w, E_t),$$

$$\mathbf{E} = (\rho u, \rho u^2 + p, \rho uv, \rho uw, (E_t + p)u + q_x),$$

$$\mathbf{F} = (\rho v, \rho vu, \rho v^2 + p, \rho vw, (E_t + p)v + q_y),$$

$$\mathbf{G} = (\rho w, \rho wu, \rho wv, \rho w^2 + p, (E_t + p)w + q_z),$$

$$\mathbf{S} = (0, f_x, f_y, f_z, Q_J - Q_R + f_x u + f_y v + f_z w),$$

$$p = R\rho T, \quad E_t = \rho\left(e + \frac{u^2}{2} + \frac{v^2}{2} + \frac{w^2}{2}\right).$$

Here, t is the time; ρ, p, and T denote the density, pressure, and temperature of gas, respectively; u, v, and w are components of the velocity vector of gas $\mathbf{v}$; E_t is the total energy per unit volume of gas; e is the internal energy per unit mass of gas; f_x, f_y, and f_z are the components of the vector of force $\mathbf{f}$ acting on gas along the coordinate axes x, y, and z, respectively; Q_J is the volumetric power of Joule dissipation, and Q_R is the power of radiation sources and sinks of energy; q_x, q_y, and q_z are components of the vector of heat flux, defined by the thermal conductivity of gas; and R is the individual gas constant.

The power of energy loss due to radiation Q_R is determined from the solution of the equation of radiative transfer,

$$\mathbf{a} \cdot \mathrm{grad}(I_\nu) = k_\nu(I_{\nu p} - I_\nu),$$

$$\mathbf{W} = \int_0^\infty d\nu \int \mathbf{a} I_\nu d\Omega, \quad Q_R = \mathrm{div}(\mathbf{W}).$$

Here, I_ν is the intensity of energy of radiation on frequency ν, $I_{\nu p}$ is the intensity of equilibrium radiation, $k_\nu(\nu, T, p)$ is the absorption coefficient, $\mathbf{a}$ is the unit vector which defines the direction of radiation for solid angle $d\Omega$, and $\mathbf{W}$ is the radiation flux density.

The electrodynamic parameters are calculated by the equation following from the system of Maxwell equations,

$$\mathrm{div}(\sigma \nabla \varphi) = \mathrm{div}(\sigma \cdot \mathbf{E}^{\mathrm{ind}}). \quad (1)$$

The induced electric field $\mathbf{E}^{\mathrm{ind}}$ is defined by the expression

$$\mathbf{E}^{\mathrm{ind}} = \mathbf{v} \times \mathbf{B}.$$

The magnetic field induction includes both the external, $\mathbf{B}_0$, and induced, $\mathbf{B}^{\mathrm{ind}}$, components,

$$\mathbf{B} = \mathbf{B}_0 + \mathbf{B}^{\mathrm{ind}}, \quad \mathbf{B}^{\mathrm{ind}} = \frac{1}{4\pi\mu_0}\int_V \frac{[\mathbf{j}(x, y, z) \times \mathbf{r}]}{r^3} dV.$$

In the electrodynamic relations, $\mathbf{j}$ is the current density, σ is the electrical conductivity of gas, and μ_0 is the magnetic constant. The solution of Eq. (1) helps find the distribution of potential $\varphi(x, y, z)$, which is used for determining the distributions of electric field intensity $\mathbf{E}(x, y, z) = -\nabla\varphi$ and current density $\mathbf{j}(x, y, z)$ using Ohm's law, as well as Joule dissipation $Q_J = j^2/\sigma$ and Lorentz force $\mathbf{f} = \mathbf{j} \times \mathbf{B}$.

A detailed description of the computational algorithm of this system of equations is found in [6]. The transport [7] and radiative [8] properties of air were introduced into the computer codes in the form of tables.

CALCULATION RESULTS

The discharge structure was calculated for the current strength of 320 A and transverse magnetic field induction of 0.086 T. The space difference grid on x, y, and z axes has dimensions of $121 \times 49 \times 25$ with steps $h_x = h_y = h_z = 0.5$ mm. For reducing the number of difference grid points on the x-axis, the frame of reference was moved in calculations with a velocity of 20 m/s in

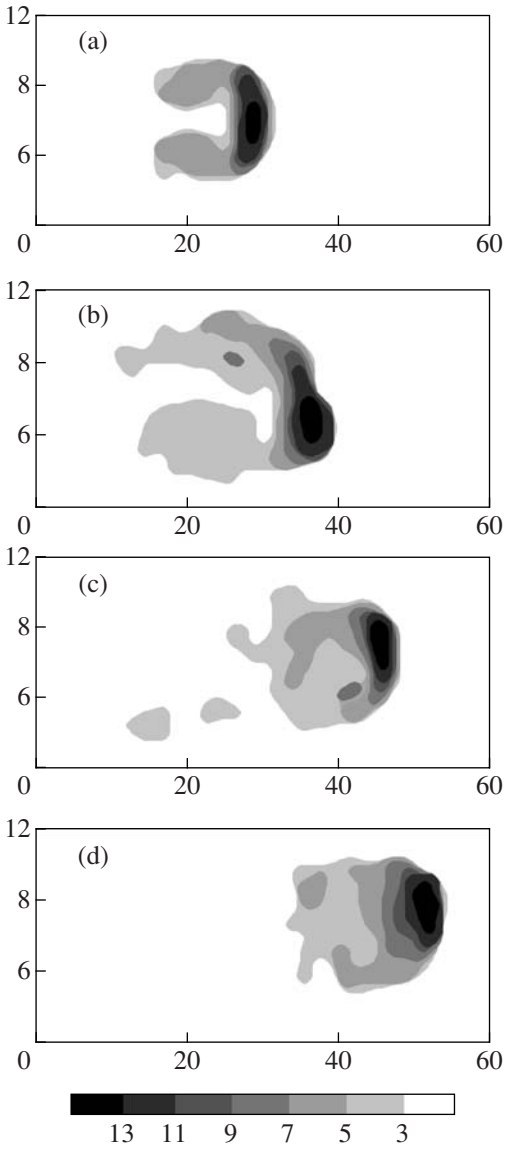

Fig. 1. The temperature distribution in the discharge midsection for the instants of time of (a) 0.3 ms, (b) 0.65, (c) 1.05, (d) 1.3. The temperature is in kK.

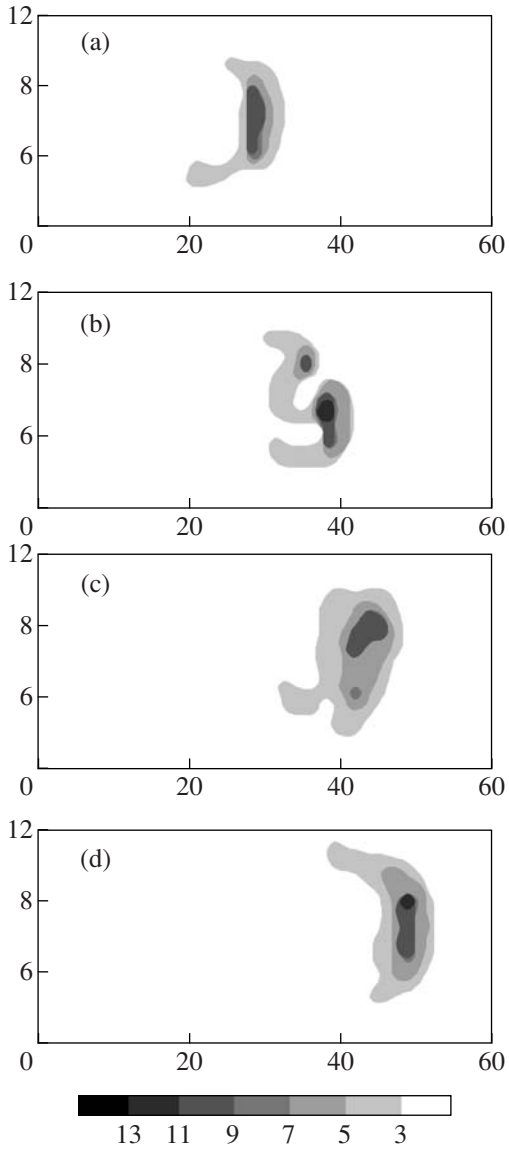

Fig. 2. The temperature distribution at the electrode for the instants of time of (a) 0.3 ms, (b) 0.65, (c) 1.05, (d) 1.3. The temperature is in kK.

the direction of discharge motion. In the initial state, the arc was preassigned as the region of hot electrically conducting gas in the form of a cylinder.

Numerical simulation involved the calculation of distributions of physical parameters and of the shape of arc discharge, which were formed as a result of force interaction with the flow and of the processes of heat transfer. Figures 1 and 2 give the distributions of temperature at the discharge center and in the electrode layer for time instants $\Delta t = 0.3$, 0.65, 1.05, and 1.3 ms. The temperature field $T(x, y)$ at the center corresponds to the midsection equidistant from both electrodes.

As a result of interaction with incident flow, the shape of highly electrically conducting region of discharge in the central part of discharge column is deformed and stretches in the transverse direction, and a sheet of gas of temperature of approximately 7×10^3 K and significantly lower electrical conductivity than that in the discharge region is carried away from the discharge edges (Fig. 1). Away from the discharge, this gas cools off and completely loses its electrical conductivity.

The thermal contraction of current-conducting column occurs in the electrode layer; in so doing, the area of current flow is reduced to the size which provides for the value of current density required for the compensation of additional power of heat flux in the direction of the electrodes (Fig. 2a). The values of temperature in this region are lower than those in the discharge column, which is due to additional energy loss. The form

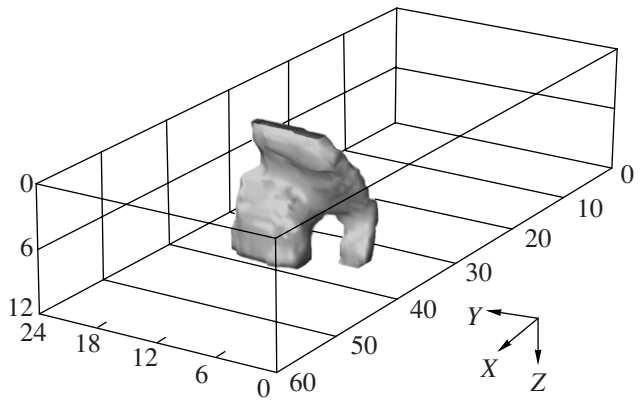

Fig. 3. The surface of constant temperature ($T = 10^4$ K) for the instant of time of 0.65 ms.

of the point of attachment varies at random throughout the process (Figs. 2b–2d), and the temperature distribution over its area is nonuniform.

Conditions for the emergence of RTI are realized throughout the height of discharge on the boundary between the arc column and incident flow; the force of gasdynamic pressure acts here on the side of cold gas of incident flow in the direction of less dense gas-discharge plasma. However, the development of instability is periodically initiated only in the electrode layers, because the discharge exhibits the least thickness here, and the temperature distribution exhibits a nonuniform "spotty" structure. The development of RTI results in the separation of a relatively small point of current attachment from the basic discharge region (Fig. 2b). With time, the separated part of the point of attachment decreases in size and cools off; in some cases, it moves away from the column under the effect of incident flow and forms a thin current-conducting channel branching off from the main discharge column. No complete separation of this channel from the discharge was observed in calculations; in all cases, a decrease in temperature and the loss of electrically conducting state was observed, because the radiation and heat-conduction losses in the thin channel are much higher. The effect of development of RTI on the main discharge column consists in that the channel separated in the vicinity of the electrode draws off a part of discharge downstream, thereby introducing disturbance into its spatial shape (Fig. 1b). Later on, when the temperature in the separated channel decreases and the electrically conducting state is lost, this cooled gas is carried by the flow downstream, and the main discharge recovers its shape with time (Figs. 1c and 1d). One can judge the effect of RTI on the space shape of discharge by the surface of constant temperature $T = 10^4$ K given in Fig. 3 for the instant of time $\Delta t = 0.65$ ms. One can see in the figure that the development of instability and separation of current-conducting channel resulted in the bending of the arc column.

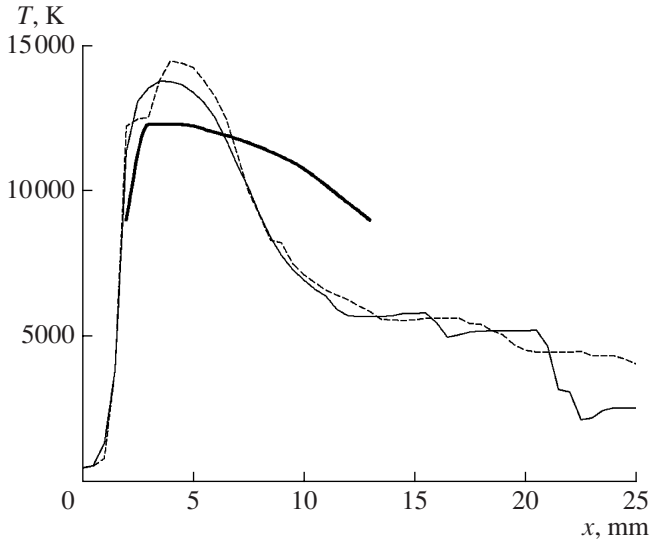

Fig. 4. The distribution of maximal temperature $T(x)$ in the discharge midsection: dashed curve—$\Delta t = 0.65$ ms, thin curve—1.3 ms, and bold curve—experiment.

For comparison with experiment, the predicted temperature dependences are constructed in the form in which the measurement data are given in [5]. Given in Fig. 4 for the instants of time $\Delta t = 0.65$ ms and 1.3 ms are the predicted dependences of maximal values of temperature $T(x)$ in the midsection plane for directions parallel with the y-axis. The x-axis points away from the direction of discharge motion, and the origin of coordinates is fixed to the front edge of discharge. The bold curve gives the experimental data. The experimentally obtained and predicted dependences are qualitatively similar; however, the prediction profiles are characterized by a higher maximal value and by a more abrupt decrease away from the center.

The temperature distribution throughout the discharge height is given in Fig. 5. The gas temperature is higher in the vicinity of the electrodes in the zone of spreading and of higher current density. At the instant of time $\Delta t = 0.65$ ms, the curve $T(z)$ has a local maximum at the central part of discharge. This is due to the fact that a side current-conducting channel separates at this point, which formed as a result of development of RTI; this caused a variation of the shape of the main discharge column and temperature disturbance. More typical of the process under investigation is the distribution corresponding to the instant of time $\Delta t = 1.3$ ms. In this case, the gas temperature decreases toward the discharge center, and its minimal value may be shifted away from the central cross section, because the pattern of temperature distribution at the point of attachment on the electrodes varies, which results in the disturbance of discharge symmetry throughout the channel height. By and large, the predicted dependence $T(z)$ adequately reflects the experimental data as regards the pattern and numerical values of temperature.

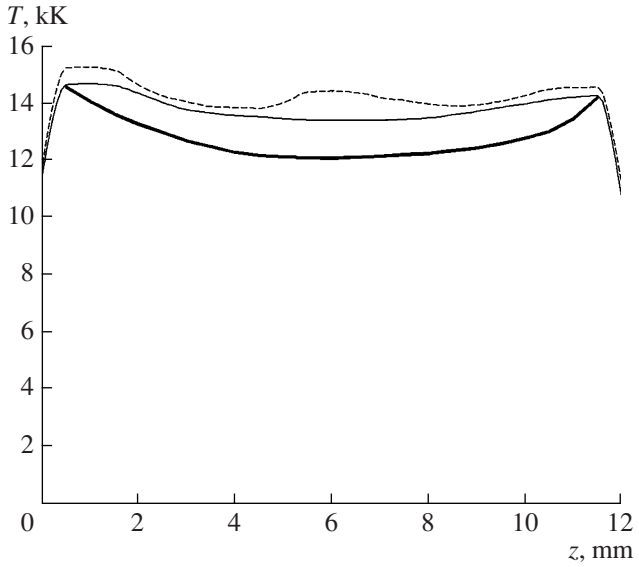

Fig. 5. The distribution of temperature throughout the channel height $T(z)$: dashed curve—Δt = 0.65 ms, thin curve—1.3 ms, and bold curve—experiment.

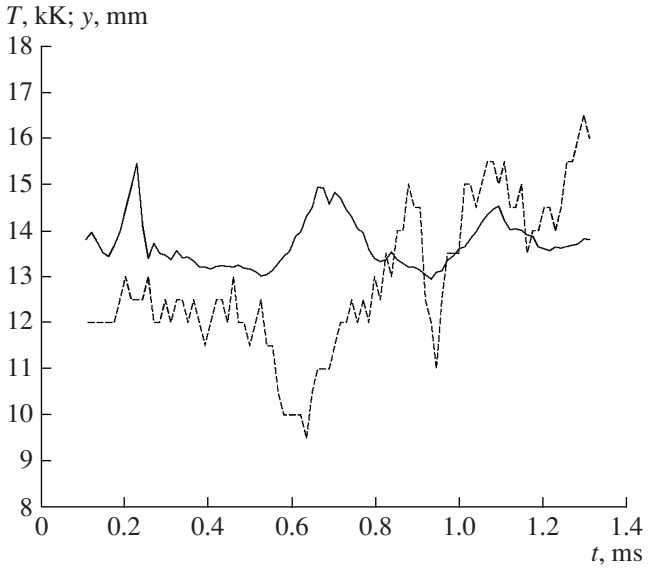

Fig. 6. Time dependences of maximal temperature T_{max} in the midsection of discharge (continuous curve) and of coordinate y corresponding to the value of T_{max} (dashed curve).

The simulation results revealed that a significantly unsteady-state process of MGD interaction is observed in the channel for the process parameters under consideration, and fluctuations of local values of physical parameters and of the discharge shape are typical of discharge. Figure 6 gives time dependences of maximal temperature T_{max} in the midsection of the discharge and of values of coordinate y corresponding to the value of T_{max}. The minimal values in $T_{max}(t)$ correspond to periods of stable burning of arc and, on the contrary, the maximal values correspond to the instants of development of RTI and of disturbance of stability. One can see in the figure that random displacement of the arc center in the transverse direction was observed during the process being simulated and that the temperature varied periodically within $(1.3–1.5) \times 10^4$ K; in so doing, the quantitative deviation from the measured value amounts to approximately 5–20%. Analysis of the process reveals that the fluctuations of temperature and shape of the arc are caused by the gas flow past the discharge column, which results in periodic vortex separation, and, even more so, by the unsteady-state processes occurring in the electrode layer. The development of RTI and the variation of the area of attachment in the electrode layer cause fluctuations of physical parameters and the disturbance of spatial shape of discharge column. Comparison calculation of this mode disregarding the heat transfer with the electrodes reveals that the level of fluctuations of parameters becomes much lower, the temperature distribution throughout the channel height levels off, and the maximal value of temperature in the central cross section is in the range $(1.26–1.28) \times 10^4$ K.

The calculation results and experimental data for the transverse dimension of the arc likewise exhibit a discrepancy. Simulation produced the shape of discharge cross section, which is extended across the channel and has a width a = 10–12 mm. In the photograph made during the experiment of [5], the width of the glow region may be estimated at approximately half the channel height, i.e., $a \approx 6$ mm. The value of discharge width in [5] was additionally determined by the distribution $\sigma(x)$ (calculated by the dependence $T(x)$) and by the value of total current; in this case, $a \approx 2$ mm was obtained. At the same time, in some studies referred to by Slovetskii [5], values of column thickness a = 10–30 mm were recorded for similar values of current strength. Apparently, the differences in the shape of arc cross section between different experiments are associated with special features of the channel and electrode structure. For example, in the considered experiment, a certain effect inhibiting the expansion of the discharge could be made by grooves on the electrodes.

Note that the dissimilarities revealed in comparing the predicted and experimentally obtained temperature distributions may be due both to the error of simulation and to the errors of measurement.

Tukhvatullin [9] gives the results of experimental investigations of temperature distribution in a plasma generator in view of spatial oscillation of the arc, which demonstrate that the arc oscillation significantly affects the results of measurements of radiation intensity and radial temperature: "It has been found that neglect of oscillation leads to underestimation of temperature in the axial part of the arc (in the investigated range of parameters up to 1500 K) and its overestimation on the periphery of the arc chamber of plasma generator (up to

2000 K).” The correction of experimental temperature distribution $T(x)$ in view of this fact will bring about a significant reduction of the difference between the measurement data and the results of numerical simulation.

CONCLUSIONS

Numerical simulation revealed that a discharge exists as a single plasma formation under conditions considered above; in so doing, heat transfer between electric-arc plasma and electrodes and the interaction with flow past the discharge column result in the emergence of spatial oscillation of the arc and temperature fluctuations.

REFERENCES

1. Kukhtetskii, S.V., Lyubochko, V.A., Mikhailenko, L.P., and Pertsev, K.V., *Zh. Prikl. Mekh. Tekh. Fiz.*, 1986, no. 1, p. 40.
2. Vasil’ev, E.N. and Nesterov, D.A., *Zh. Prikl. Mekh. Tekh. Fiz.*, 2005, vol. 46, no. 6, p. 5.
3. Sebald, N., *Appl. Phys.*, 1980, vol. 21, p. 221.
4. Vasil’ev, E.N. and Nesterov, D.A., *Teplofiz. Vys. Temp.*, 2007, vol. 45, no. 2, p. 165 (*High Temp.* (Engl. transl.), vol. 45, no. 2, p. 138).
5. Slovetskii, D.I., *Teplofiz. Vys. Temp.*, 1967, vol. 5, no. 3, p. 401.
6. Vasil’ev, E.N. and Nesterov, D.A., *Vychisl. Tekhnol.*, 2005, vol. 10, no. 6, p. 13.
7. Sokolova, I.A., *Zh. Prikl. Mekh. Tekh. Fiz.*, 1973, no. 2, p. 80.
8. Avilova, I.V., Biberman, L.M., Vorob’ev, V.S. et al., *Opticheskie svoistva goryachego vozdukha* (Optical Properties of Hot Air), Moscow: Nauka, 1970.
9. Tukhvatullin, R.S., Radiations and Temperature Fields in Gas-Discharge Plasma, *Extended Abstract of Doctoral (Tech.) Dissertation*, Kazan: KGTU im. A.N.Tupoleva (Tupolev Kazan State Technical Univ.), 2007.